Available online at www.sciencedirect.com

ScienceDirect

journal homepage: http://www.elsevier.com/locate/acme

Original Research Article

Optimization of pre-structuring parameters in fabrication of magnetorheological elastomer

Ngoc Thien Lai, Hanafi Ismail, Mohd Khalil Abdullah, Raa Khimi Shuib *

School of Materials and Mineral Resources Engineering, USM Engineering Campus, Universiti Sains Malaysia, Nibong Tebal, Pulau Pinang, 14300, Malaysia

ARTICLE INFO

Article history:
Received 8 June 2018
Accepted 23 December 2018
Available online 25 January 2019

Keywords:
Magnetorheological elastomer
Pre-structuring process
Dynamic properties
Taguchi method

ABSTRACT

Pre-structuring of magnetic particles during fabrication of magnetorheological elastomer (MRE) is a crucial step, which results in the formation of chain-like columnar structures in the rubber matrix. In this study, MRE based on natural rubber and carbonyl iron particles were prepared. The Taguchi method was utilized to study the effect of several dominating factors during the fabrication process such as pre-curing time, pre-curing temperature and applied magnetic field during curing on the loss tangent (tan δ) and tensile properties. Tan δ was measured through parallel-plate rheometer over a frequency range of 1–100 Hz and a strain amplitude range of 0.1–6%. Tensile properties were measured with a universal tensile testing machine. The obtained data were statistically analyzed using S/N ratios and ANOVA in order to predict the optimal combination of factors, and then further experiments were conducted for verification purpose. Results indicated that the magnetic field had the greatest influence on tan δ when measured over a range of frequency and elongation at break. Furthermore, pre-curing time and magnetic field were found to influence tan δ when measured over a range of strain amplitude. However, none of the factors exhibited significant influence on tensile strength. In addition, the morphology of MRE was examined using scanning electron microscopy (SEM).

1. Introduction

Rubber is by far the most commonly used materials for energy absorption and vibration control. Although rubber has proved useful in vibration damping, its low stiffness and toughness hinder its wide usage in practical applications [1]. Incorporation of metallic or ceramic particles in a rubber provides potential for improving mechanical properties of the material without sacrificing its damping performance. More recently, magnetically permeable metallic and ceramic particles (such as iron and ferrite) have been included in rubber to create elastomeric magnetic composites, resulting in improvement of damping performance as well as structural properties [2,3]. Generally, combinations of rubber with magnetic particles are termed magnetorheological elastomers (MREs) or magnetoelastic rubber or elastomer-ferromagnetic composites [4].

* *Corresponding author.*
E-mail address: raa_khimi@hotmail.com (R.K. Shuib).

https://doi.org/10.1016/j.acme.2018.12.010

MREs can be fabricated either with or without a magnetic field. The former results in isotropic MREs, while the latter results in anisotropic MREs. Isotropic MREs can be characterized by a uniform magnetic particle distribution in the matrix. Anisotropic MREs have a special chain-like columnar structure of magnetic particles in the matrix as a result of curing the materials under an applied magnetic field [5–7]. Fig. 1 shows the schematic structures of isotropic and anisotropic MREs. Anisotropic MREs are known to produce materials with much larger vibration damping and stiffness [8,9] compared to those cured in the absence of a magnetic field. Here the damping is mainly promoted by the viscoelastic damping and interfacial damping [8] as do conventional rubber dampers, but inclusion of magnetic particles in the rubber enables additional damping through magnetism-induced damping [10].

A number of elastomers have been utilized as matrices for MREs, including silicone rubber [11–13], natural rubber [10,14,15], styrene butadiene rubber, chloroprene rubber, bromobuthyl rubber, cis-polyisoprene [16], thermoplastic elastomers such as polyurethane [17,18] and several copolymers [16,19]. Typical magnetic particle of choice for MREs is carbonyl iron particles. Intended for peculiar uses, carbonyl iron can be mixed with or replaced by other magnetizable particles such as nickel zinc ferrite, barium hexaferrite or strontium ferrite [16]. Some of these alloy particles actually perform better than carbonyl iron, but they are significantly more expensive.

In this study, natural rubber was chosen as the matrix because it is the commonly used matrix materials in most recent studies and it is easy to process, has highest failure strain of any rubber and is unbeatable in terms of damping performance [2,20,21]. Carbonyl iron was selected as the magnetic particles because of their spherical shape, high permeability and high saturation magnetization [16]. However, the performance of MREs depends not only on the matrix and type of magnetic particles, but also on the columnar structures in anisotropic MREs. The technique to align the magnetic particles into chain-like structures in the rubber matrix is known as pre-structuring process. There are three main factors that affect the pre-structuring process; pre-structuring time, pre-structuring temperature and applied magnetic field [8,13,22]. In this process, uncured MRE samples are placed for a period of time at elevated temperature under an applied magnetic field. In instances where magnetic particles are exposed to an applied magnetic field, the magnetic dipole of each particle is aligned along the field direction. Influenced by the magnetic force, the north pole of each particle is attracted to the south pole of the one next to it, resulting in the formation of chains and columnar structures inside the matrix. Upon final curing of the matrix, the particle chains are locked in place [5]. Although several works have been carried out to investigate factors influencing pre-structuring process of MREs, none have assessed the optimum combined effect of these factors to ensure the high performance of final products.

The conventional factorial design can be used to study optimum combination effect of multiple factors. However, as the number of factors increases, the multi-level factorial design becomes infeasible due to large number of experimental runs, high costing and time consuming. In order to reduce the number of experiments to a practical level for experimental involving multiple factors, the Taguchi method can be employed to screen out the important factors from and optimize combination of factors to achieve high quality product and process. This work aims to assess the effects of a number of factor during pre-structuring process, namely, pre-structuring time, pre-structuring temperature and applied magnetic field during curing on loss tangent (tan δ) and tensile properties of the MREs using Taguchi experimental design method. Tan δ gives a comparison of the energy lost to that stored; it is obtained by dividing the loss modulus (G'') by the storage modulus (G'). In this study the tan δ was measured in passive mode which could be potentially reliable for fabrication of passive damping devices such as seismic bearing and engine mounting. Tensile properties were measured using universal tensile tester.

2. Experimental

2.1. Materials

Compounding formulation used in this study is shown in Table 1. Natural rubber and all other chemicals listed in Table 1 were supplied by Zarm Scientific & Supplies Sdn. Bhd, Malaysia. Carbonyl iron particles (CIP) were purchased from

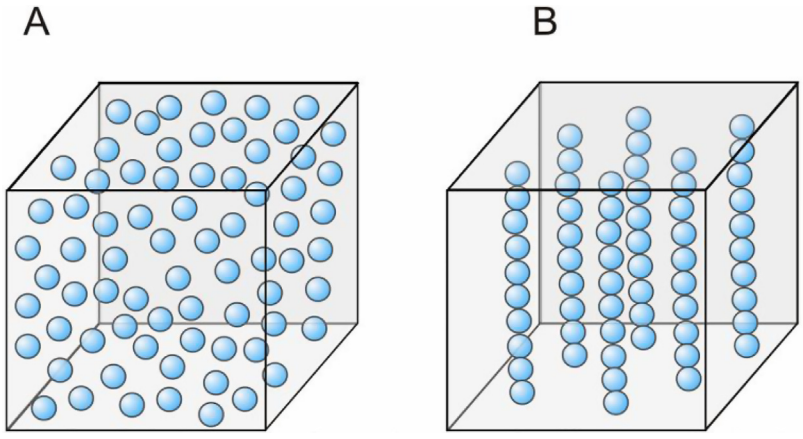

Fig. 1 – Schematic structure of (A) isotropic and (B) anisotropic MREs [5].

Table 1 – Compounding formulation.

Materials	Functions	Content (phr)[a]
Natural rubber (SMR L)	Matrix	100
Zinc oxide	Activator	5
Stearic acid	Activator	1
Paraffin oil	Plasticizer	5
Carbonyl iron	Magnetic particles	70
N-isopropyl-N′-phenyl-1,4-phenylenediamine (IPPD)	Antioxidant	2
N-cyclohexyl-2-benzothiazole sulfenamide (CBS)	Accelerator	2
Tetramethylthiuram disulfide (TMTD)	Accelerator	1
Sulfur	Crosslinking agent	1.5

[a] part per hundred by weight of the rubber.

Table 2 – Experimental factors and their levels.

Factors	Unit	Level 1	Level 2	Level 3	Level 4
Pre-curing time (*t*)	min	3	5	10	15
Pre-curing temperature (*T*)	°C	60	80	100	110
Magnetic field (*M*)	mT	0	100	150	165

Shanghai YY International Co., Ltd., China. Characterization of the particles thorough scanning electron microscopy (SEM) and laser diffraction analysis revealed that particles had a spherical morphology with an average diameter of 4 μm.

Design of experiments

The Taguchi method, pioneered by Genichi Taguchi, provides a simple and efficient, approach to study the effects of multiple factors by identifying the performance trend for each factor and determining the combination that yields the optimum conditions. In general, the Taguchi method includes the following steps: (a) determination of the factors and their respective levels, (b) design of experiments using an appropriate orthogonal array (OA), (c) conducting of experiments, (d) analysis of data and selection of the optimum level for each factor, and (e) confirmatory tests of the optimum condition. The brief overview and details procedure to implement those steps are published in Ref. [23].

In this study, three factors affecting the pre-structuring process were selected: pre-curing time (*t*), pre-curing temperature (*T*) and applied magnetic field during pre-curing and curing (*M*). These factors were varied at four different levels as presented in Table 2.

L'16, the smallest appropriate OA for three factors and four levels, was selected for the Taguchi method. Table 3 shows the experimental layout of the L'16 OA according to the Taguchi method with 16 rows corresponding to 16 trials and three columns representing three factors with their respective levels. The S/N ratios were subsequently used to analyze the results. In this work, larger-is-better target for S/N ratios was selected. The STATISTICA software was utilized to perform ANOVA and to evaluate the percentage contribution of each factor.

2.2. *Fabrication of MREs*

The compound formulation in Table 1 was compounded using a conventional laboratory two-roll mill (XK 160) according to ASTM D3184-07. Rubber was first softened (masticated) in the two-roll mill for 2–3 min. Activators, plasticizer and carbonyl iron particles were then added, whereas accelerators and sulfur were added before the end of compounding process in order to avoid premature vulcanization. The mixing time was kept constant at approximately 30 min. The cure time at 150 °C was determined by an Alpha MDR2000 moving die rheometer according to D6204-15. Compounded rubber samples of approximately 40 g were placed in a 120 mm × 65 mm × 3 mm mold. Subsequently, the compounded rubber samples were pre-structured in a compression molder (SH-48-100-PLC) equipped with adjustable temperature feature at the respective pre-cure time, pre-cure temperature and magnetic field according to the OA in Table 3. The magnetic field was induced by a specially developed magnetic mold as shown in Fig. 2. The magnetic field was varied by adjusting the gap between top and bottom mold using different thickness of metal plates and the magnetic field strength was measured using KANETEC TM-

Table 3 – Experimental layout for L'16 OA according to the Taguchi method.

Trials	Factors and their levels		
	t	*T*	M
1	1	1	1
2	1	2	2
3	1	3	3
4	1	4	4
5	2	1	2
6	2	2	1
7	2	3	4
8	2	4	3
9	3	1	3
10	3	2	4
11	3	3	1
12	3	4	2
13	4	1	4
14	4	2	3
15	4	3	2
16	4	4	1

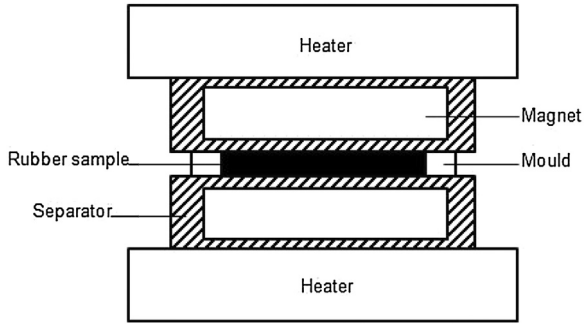

Fig. 2 – Schematic diagram of pre-structuring process.

801 Tesla meter. After pre-structuring process, MREs were cured at 150 °C under a pressure of approximately 10 MPa. The magnetic field was maintained throughout the curing of anisotropic MREs.

2.3. *Characterization*

2.3.1. *Morphology*

The fractured surface of MREs were observed using a Hitachi TM3000 scanning electron microscope (SEM). Surfaces were coated with a thin layer of gold prior to observation at an accelerating voltage of 15 kV.

2.3.2. *Dynamic mechanical analysis*

The influence of frequency and amplitude strain on tan δ was examined using an Anton Paar MCR 301 Parallel Plate Rheometer on circular specimens of 20 mm diameter and 3 mm thickness in shear mode at room temperature according to ASTM D5992. Tan δ was measured over a frequency range of 1–100 Hz with a fixed strain amplitude of 2% and over a strain amplitude of 0.1–6% with a fixed frequency of 10 Hz. Each test was repeated three times.

2.3.3. *Tensile test*

Tensile test was performed on dumbbell-shaped specimens using an Instron 3366 universal tensile testing machine at a crosshead speed of 500 mm/min according to ASTM D412-16. Tensile strength, elongation at break and M100 were measured and analyzed. Each test was repeated three times.

3. Results and discussion

3.1. *Morphology*

Fig. 3 shows SEM images of isotropic and anisotropic MRE samples. From SEM images, it can be clearly seen that isotropic MREs have a uniform distribution and dispersion of carbonyl iron with no obvious aggregation in the rubber matrix. For anisotropic MREs, clearly, as expected, curing the material under an applied magnetic field at elevated temperature allowed the particles to organize into chain-like structures.

3.2. *Dynamic mechanical properties*

In order to calculate the optimum level for each factor, reference points for tan δ were selected for S/N ratios and ANOVA analysis. The maximum value of tan δ, constantly observed at 15.8 Hz, was selected as the reference point in order to optimize the tan δ over a range of frequency from 1 to 100 Hz. Furthermore, to optimize tan δ over a range of strain amplitude from 0.1 to 6%, the maximum value of tan δ, constantly observed at 6% strain amplitude, was selected as the reference point. In tensile testing, ultimate tensile strength and elongation at break were selected as reference points to calculate the optimum level of each factor for tensile properties.

Table 4 shows the values of tan δ, ultimate tensile strength and elongation at break obtained from the reference points. Each value represents an average from three tested samples. The highest value for each measured parameter has been shown in bold.

3.3. *Effect of frequency on tan δ*

Fig. 4 shows the main effect plots of the influence of frequency on tan δ when the factors were varied at four different levels. As discussed in reference [23], higher value of S/N ratio indicates better signal, which signifies that the highest value of S/N ratio could be used to obtain the highest tan δ. Taguchi method suggested that an optimized value for tan δ could be

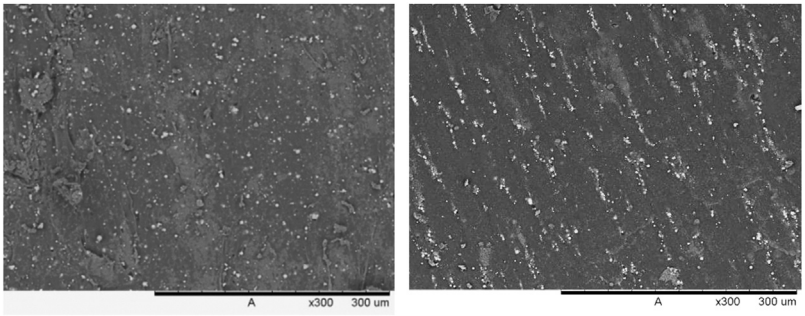

Fig. 3 – SEM images of (a) isotropic MRE and (b) anisotropic MRE.

Table 4 – Tan δ and tensile test results used to calculate S/N ratios and ANOVA.

Sample type	Maximum tan δ over 1–100 Hz frequency (15.8 Hz, strain amplitude = 2%)	Maximum tan δ over 0.1–6% strain amplitude (6%, frequency = 10 Hz)	Tensile strength (MPa)	Elongation at break (%)
1	0.054	0.105	12.60	**808.89**
2	0.156	0.318	10.37	642.22
3	0.144	0.291	12.53	710.56
4	0.191	0.283	11.02	619.44
5	0.109	0.300	2.44	285.56
6	0.083	0.382	12.03	752.22
7	0.111	0.126	12.56	710.56
8	0.094	0.117	11.10	643.89
9	0.228	0.500	2.95	345.56
10	0.147	0.430	8.96	643.33
11	0.051	0.180	11.09	766.11
12	**0.270**	**0.509**	9.13	582.78
13	0.223	0.317	12.54	742.22
14	0.151	0.173	11.16	623.89
15	0.137	0.335	10.45	681.11
16	0.059	0.310	**12.92**	726.11

obtained if the pre-structuring process was carried out at 10 min., 110 °C and 165 mT magnetic field. As displayed in Fig. 4(a), the S/N ratio increased with increasing pre-curing time until it reached a maximum value at 10 min, thereafter, slightly decreased at the longest pre-curing time. The increase of S/N ratio with increasing pre-curing time could be explained by the increase of the degree of freedom of movement for carbonyl iron to align and form columnar structures during pre-structuring process and the reaching of a saturation stage after 10 min. It was observed that, further increasing of pre-curing time does not significantly affect the alignment of carbonyl iron in the rubber matrix. Similar findings have been reported by Li et al. [13]. As can be seen from Fig. 4(b), the pre-curing temperature had minimal influence on S/N ratios, but the S/N ratio at 110 °C was the highest. At 110 °C, the viscosity of the matrix reduced, which softened the rubber and allowed

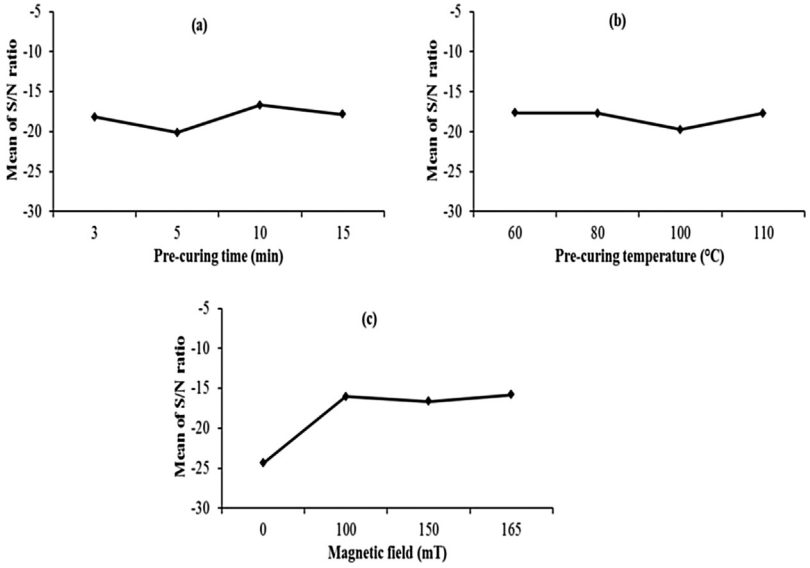

Fig. 4 – Main effect plots for S/N ratio of tan δ at 15.8 Hz: (a) effect of pre-curing time, (b) effect of pre-curing temperature and (c) effect of the magnetic field during curing.

Table 5 – ANOVA results and factor significance for tan δ at 15.8 Hz.

Factor	Sum of squares	Degree of freedom	Confidence level (%)	Percentage contribution (%)	Factor significance ($S/N_{max} - S/N_{min}$)
Time (min)	0.050	3	99.99	28.41	3.45
Temperature (°C)	0.012	3	99.86	6.82	2.13
Magnetic field (mT)	0.114	3	99.99	64.77	8.55

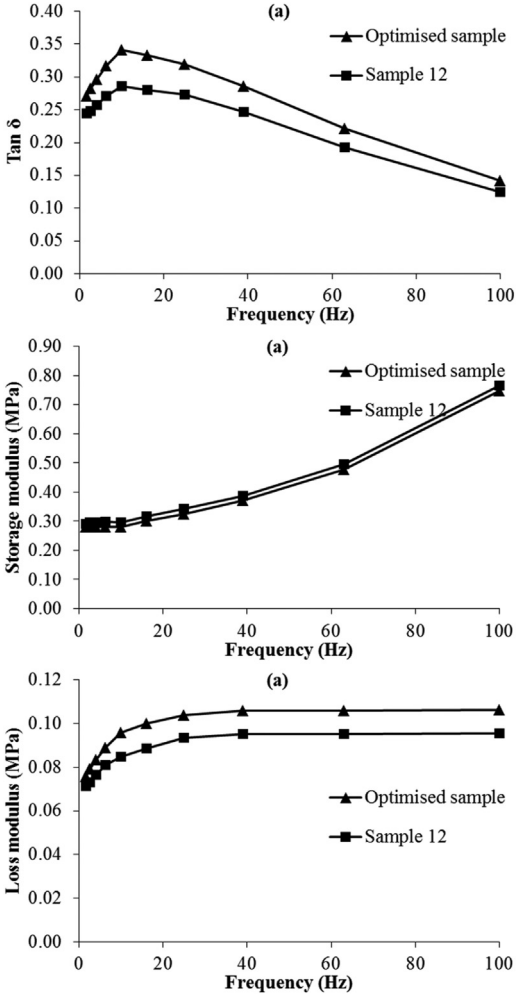

Fig. 5 – (a) tan δ, (b) storage modulus and (c) loss modulus versus frequency for the optimized sample and sample 12.

the magnetic particles to be organized into chain-like structures. As displayed in Fig. 4(c), the S/N ratios for anisotropic MRE (cured at 100 mT, 150 mT and 165 mT) were higher compared to that of isotropic MRE (cured at 0 mT). This indicated that formation of magnetic particle chains and columnar structures provided additional damping through magnetism-induced damping [24].

Table 5 shows ANOVA results for the effect of frequency on tan δ. It can be seen that the variability for each factor was tested at 99.9% confidence level. Apparently, the magnetic field during pre-curing had the greatest influence on tan δ at 15.8 Hz, followed by pre-curing time and pre-curing temperature. It was also apparent that pre-curing temperature had much less influence, with a contribution less than 10%. The greatest influence of magnetic field on tan δ could be explained due to increase energy absorbed to overcome interparticle magnetic interaction; these processes transform elastic energy into magnetic energy which subsequently dissipates by magnetic hysteresis [25].

The final and crucial step in the Taguchi method was to conduct confirmatory experiments to verify the predicted optimum conditions. The optimized sample was prepared at 10 min pre-structuring time, 110 °C and 165 mT magnetic field. The tan δ value was compared to the highest value previously attained (sample 12). The variation of tan δ with frequency for optimized sample and sample 12 is displayed in Fig. 5(a). It was found that tan δ was higher for the optimized sample over the entire examined frequency range. This supported the optimum conditions suggested by S/N ratios and ANOVA. G' and G'' were also plotted in Fig. 5(b) and (c) to assist in explaination of the mechanism involed in the changes in tan δ. It can be seen that the increase of tan δ for optimized sample was primarily a result of the increase of G'' rather than G'. The increase in G'' could be explained by the increase in total energy dissipated by viscoelastic damping of the rubber matrix, interfacial damping

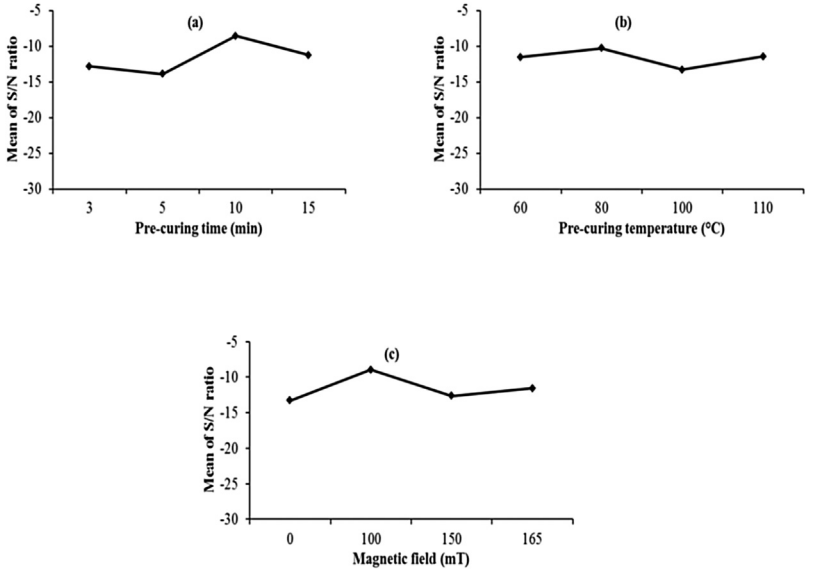

Fig. 6 – Main effect plot for S/N ratio of tan δ at 6% strain amplitude: (a) effect of pre-curing time, (b) effect of pre-curing temperature and (c) effect of the magnetic field during curing.

Table 6 – ANOVA results and factor significance for tan δ at 6% strain amplitude.

Factor	Sum of squares	Degree of freedom	Confidence level (%)	Percentage contribution (%)	Factor significance ($S/N_{max} - S/N_{min}$)
Time (min)	0.220	3	99.99	58.01	5.36
Temperature (°C)	0.060	3	99.89	15.83	3.02
Magnetic field (mT)	0.099	3	99.98	26.12	4.34

by friction at the interface between carbonyl iron and rubber as well as magnetism-induced damping.

3.4. *Effect of strain amplitude on tan δ*

Fig. 6 shows main effect plots of the S/N ratios for the influence of strain amplitude on tan δ. The highest values of S/N ratios were obtained at 10 min pre-curing time, 80 °C and 100 mT magnetic field. As shown in Fig. 6(a), the S/N ratio increased with increasing pre-curing time to 10 min and slightly decreased at 15 min. This is similar to the effect of frequency on tan δ and suggested that the time saturation for carbonyl iron particles aligned in the rubber matrix occurred at 10 min. It should be noted that in this study, the suggested optimum conditions for pre-curing temperature and magnetic field were different from those for the effect of frequency on tan δ. A lower pre-curing temperature at 80 °C was found to be sufficient to soften the rubber matrix, which allowed the carbonyl iron particles to be organized into chain-like structures. This is in agreement with findings reported by Chen et al. [8]. As can be seen in Fig. 6(c), tan δ for samples cured under magnetic field were also higher compared to those cured without a magnetic field. This could again be explained due to additional energy absorbed to overcome magnetic interaction between neighboring particles [26].

Table 6 illustrates ANOVA results for the effect of strain amplitude on tan δ. It can be seen from the level of contribution that pre-curing time had the greatest influence on tan δ with 99.99% confidence level, followed by magnetic field also with 99.99% confidence level. The influence of pre-curing temperature was much lower at 15.83%. As was the case for the effect of strain amplitude on tan δ here, it should also be noted that the contribution of magnetic field was lower than pre-curing time, which was different compared with the contributions for the effect of the frequency on tan δ (magnetic field = 65% and pre-curing time = 28%). The different contributions for different tests suggested that for the experiment on the effect of the strain amplitude on tan δ, the energy loss was more dominated by the viscoelastic damping of the rubber matrix and interfacial friction of carbonyl iron and rubber compared with magnetism-induced damping. It is worth mentioning here that, an increase in magnetic field during curing at elevated temperature which produced longer chain like columnar structures and lead to increase in strain energy during loading and stiffness of the MREs might not influence the decrease of magnetic field contribution to the tan δ due to energy loss per cycle is proportional to the square of the strain amplitude. However, formation of longer particle chains opposed the higher shearing force with increasing strain amplitudes, such that the particle chain orientation changed and transformed elastic energy into magnetic energy, which then dissipated by magnetic hysteresis [25].

Verification experiment was carried out at the optimized pre-structuring conditions: 10 min, 80 °C and 100 mT. As can be seen from the results for tan δ, the value obtained for the optimized sample was slightly higher compared to the highest value previously attained (sample 12). Figure 7 shows tan δ, G′

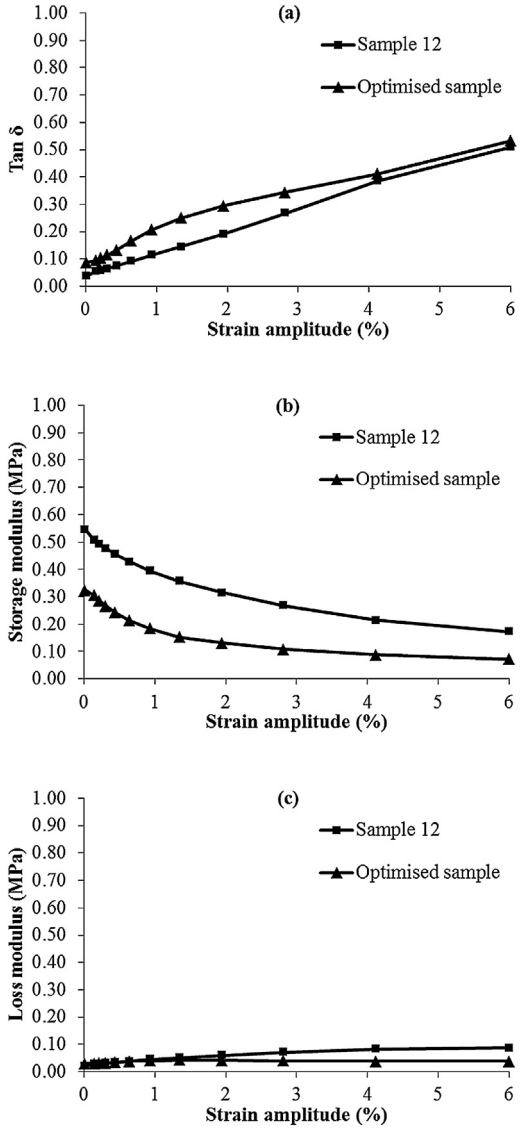

Fig. 7 – (a) tan δ, (b) storage modulus and (c) loss modulus versus strain amplitude for the optimized sample and sample 12.

and G'' for the optimized sample and sample 12 over a 0.1–6% range of strain amplitude. It was observed that tan δ increased with increasing strain amplitude, while the increment of tan δ was mainly due to the decrease in G' as opposed to G''. The decrease in G' could be attributed to the Payne effect [27]. This effect can be explained by the disintegration of filler aggregates which releases trapped rubber and allows additional rubber to take part in energy dissipation, the separation of dipole–dipole interaction between neighboring particles, and filler–rubber detachment and reformation that increases with increasing strain amplitude.

3.5. *Tensile properties*

The main effect plots of the S/N ratios for the ultimate tensile strength are depicted in Fig. 8. The obtained results suggested that the highest value of tensile strength might have been obtained by pre-curing the samples at 15 min, 100 °C and 0 mT magnetic field. However, no obvious trend of the S/N ratios was observed for any factor as the levels changed. It was also noted that the suggested pre-curing time and temperature to obtain the highest tensile strength were similar to those for the optimum conditions when assessing the influence of frequency and strain amplitude on tan δ. This was further supported that the temperature required to soften the rubber matrix should be above 80 °C and the time required for the particles to align into chain-like columnar structures should be approximately 10–15 min. However, the suggested optimum magnetic field during pre-curing led to a contradictory conclusion where the samples which were cured without a magnetic field had higher tensile strength compared to those cured under a magnetic field. This could be explained by the different modes

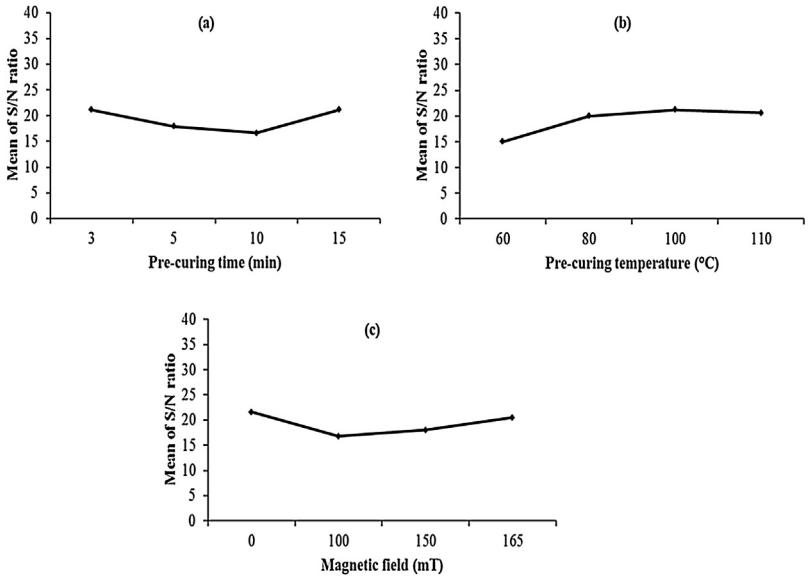

Fig. 8 – Main effect plots for S/N ratios of ultimate tensile strength: (a) effect of pre-curing time, (b) effect of pre-curing temperature and (c) effect of the magnetic field during curing.

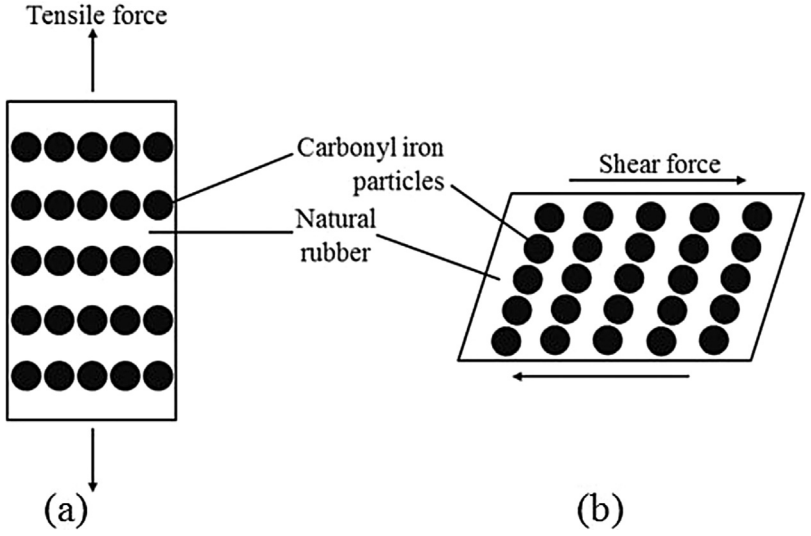

Fig. 9 – Effect of (a) tensile mode and (b) shear mode on particle separation.

Table 7 – ANOVA results for tensile strength.

Factor	Sum of squares	Degree of freedom	Confidence level (%)	Percentage contribution (%)	Factor significance ($S/N_{max} - S/N_{min}$)
Time (min)	115.522	3	99.99	32.99	1.50
Temperature (°C)	115.222	3	99.99	32.99	2.07
Magnetic field (mT)	119.963	3	99.99	34.02	1.60

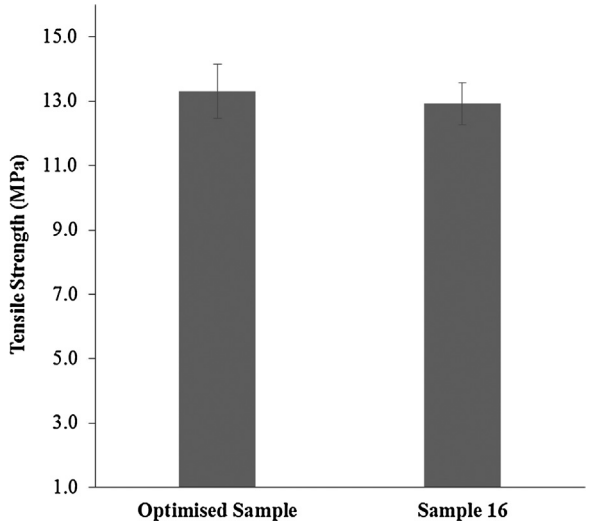

Fig. 10 – Tensile strength for the optimized sample and sample 16.

of loading which were used during testing (tensile versus shear). This implied that reinforcement effect provided by the formation of magnetic particle alignment in the rubber matrix was less efficient in tensile mode in comparison to the shear mode performed using parallel plate rheometer. This was not surprising, given that in tension, it was solely the spacing between chains that was increased, whereas in shear the spacing between neighboring particles within chains was increased (see Fig. 9). This is in agreement with similar findings reported by Wang et al. [28]. In addition, it is possible to improve reinforcement effect of magnetic particle alignment in tensile mode by fabrication of MREs with magnetic particle align parallel to tensile direction. However, further work would be needed to assess that.

Table 7 illustrates the ANOVA results for ultimate tensile strength of MREs. The variability for each factor was tested at 99.99% confidence level. It was observed that none of the factors had a significant influence on tensile strength and the percentage contribution was approximately the same for each factor.

Fig. 10 compares the tensile strength for the sample at the suggested optimum conditions (15 min, 100 °C and 0 mT) to the highest tensile strength previously achieved in sample 16. Tensile strength for the optimized sample and sample 16 were 13.305 MPa and 12.924 MPa, respectively. This supported the optimum conditions suggested by the S/N ratios and ANOVA. As can be seen, the pre-structuring parameters for the optimized sample and sample 16 were similar and both suggested that curing the material without an applied magnetic field resulted in higher tensile strength. This could again be explained due to the different modes of loading during testing. Furthermore, curing the samples without a magnetic field caused a uniform suspension of magnetic particles in the rubber matrix, which increased the efficiency of stress transfer

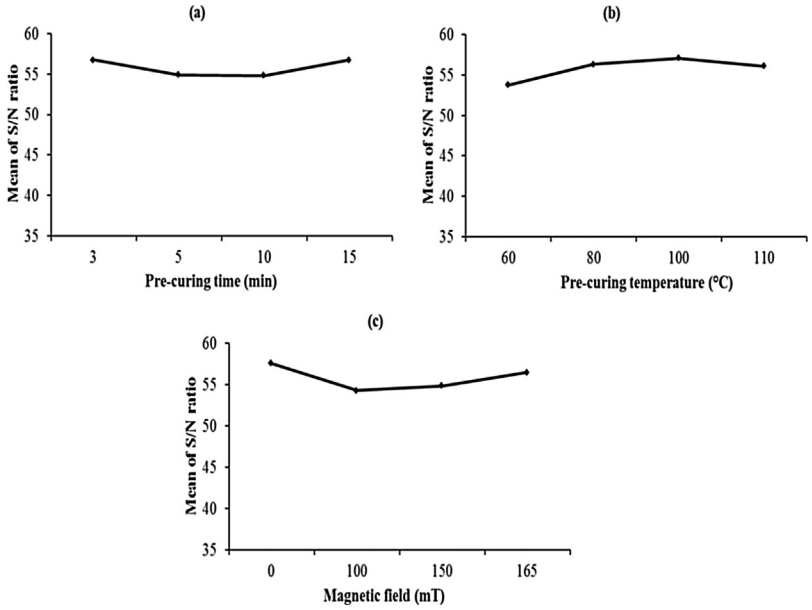

Fig. 11 – Main effect plots for S/N ratios of elongation at break: (a) effect of pre-curing time, (b) effect of pre-curing temperature and (c) effect of magnetic field during curing.

Table 8 – ANOVA Table and factor influence for elongation at break.

Factor	Sum of squares	Degree of freedom	Confidence level (%)	Percentage contribution (%)	Factor significance ($S/N_{max} - S/N_{min}$)
Time (min)	128,579.26	3	99.99	19.53	0.65
Temperature (°C)	185,832.80	3	99.99	28.23	3.33
Magnetic field (mT)	343,874.08	3	99.99	52.24	3.33

between particles and matrix, resulting in enhancement of stiffness, strength and failure strain of the material.

The main effect plots of the S/N ratios for elongation at break are presented in Fig. 11. As expected, the suggested optimum conditions to obtain highest elongation at break were similar to those for the optimum conditions to obtain highest ultimate tensile. The Taguchi method suggested that the highest elongation at break and tensile strength could be obtained at 15 min pre-curing time, 100 °C and 0 mT magnetic field. Moreover, it can be noted that no significant trend of S/N ratios was observed for any factor as the level varied. Similar to the tensile strength, elongation at break for samples cured without a magnetic field was also higher than those cured under an applied magnetic field. This could be explained due to better interfacial interaction in isotropic MREs, in which the particles were dispersed uniformly and the rubber chains tended to coil around the particles, which allowed them to uncoil and re-align along the stress direction when stretched. Wang et al. have reported similar findings in Ref. [28].

Table 8 shows ANOVA results for elongation at break. The confidence level for all factors was 99.99%. From the level of contribution, it can be seen that the most influential factor was magnetic field, which was related to the curing the material in the absence of a magnetic field. The effect of pre-curing time and temperature was observed to be less significant at 19.53% and 28.23%, respectively.

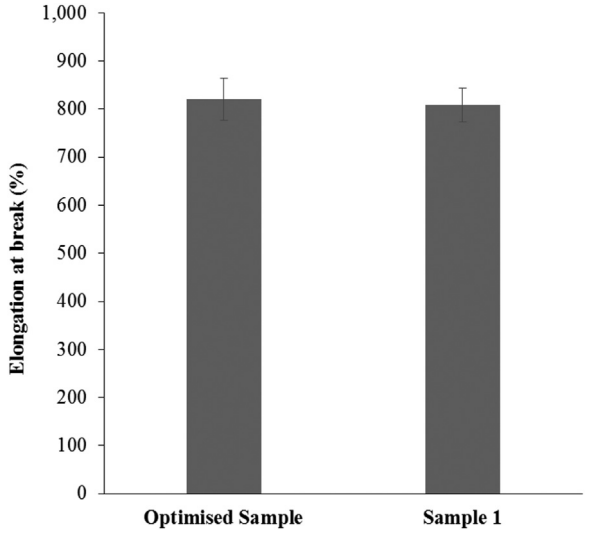

Fig. 12 – Elongation at break for the optimized sample and sample 1.

Fig. 12 shows elongation at break for the optimized sample and the highest elongation at break previously achieved (sample 1). As expected, elongation at break for the optimized sample (820.167%) was slightly higher compared to sample 1 (808.889%). This supported the optimum conditions suggested by the Taguchi method and ANOVA. As stated, both samples were pre-structured without the presence of a magnetic field and the results yet again revealed that homogenous distribution of particles in the matrix improved the elongation at break of the material. Furthermore, uniform distribution of particles allowed the rubber molecular chains to slide against each other more easily and reduced the stress concentration which might have led to premature breakdown of the sample.

4. Conclusion

In this study, MREs based on natural rubber and carbonyl iron particles were fabricated. Experiments were designed using Taguchi method to assess the combined influence of three pre-structuring factors, namely pre-curing time, pre-curing temperature, and magnetic field on dynamic mechanical and tensile properties of MREs. SEM micrographs revealed that without a magnetic field, carbonyl iron particles were uniformly distributed in the rubber matrix, while an applied magnetic field at elevated temperature led to the formation of chain-like structures. The optimum conditions suggested by the Taguchi method for the effect of frequency on tan δ were 10 min, 110 °C, and 165 mT magnetic field; these were verified by the experiment. ANOVA results revealed that magnetic field during curing had the greatest influence on tan δ, followed by pre-curing time, and pre-curing temperature. The suggested optimum conditions to obtain the highest tan δ for the influence of strain amplitude were similar to those when assessing the influence of frequency on tan δ, while the optimum conditions suggested by the Taguchi method were 10 min, 80 °C, and 100 mT. Furthermore, pre-curing time was found to have the greatest influence on tan δ, followed by magnetic field, and pre-curing temperature. The Taguchi method suggested that the optimum pre-structuring conditions to obtain the highest tensile strength and elongation at break were 15 min, 100 °C, and 0 mT. The pre-curing time and temperature were comparable with the suggested optimum conditions to obtain the highest tan δ. However, the applied magnetic field was different, which could have been due to the different mode of testing (tensile versus shear). The different optimum pre-structuring conditions for different tests could be due to the relatively varied degrees that various mechanisms possessed with different loading conditions and different testing parameters. It is considered that the

suggested Taguchi parameters investigated in this study can provide a guideline to manufacture MREs using different types of matrix materials with desired formation of chain like columnar structures and damping performance.

Conflict of interest

The authors declare there are no conflicts of interest to disclose.

Acknowledgements

The authors gratefully acknowledge support from the Universiti Sains Malaysia and the School of Materials and Mineral Resources Engineering. This project was funded by Ministry of Education Malaysia through the FRGS grant 203/PBAHAN/6071349.

REFERENCES

[1] M. Brodt, R.S. Lakes, Composite materials which exhibit high stiffness and high viscoelastic damping, J. Compos. Mater. 29 (1995) 1823–1833.
[2] J. Yao, Y. Sun, Y. Wang, Q. Fu, Z. Xiong, Y. Liu, Magnet-induced aligning magnetorheological elastomer based on ultra-soft matrix, Compos. Sci. Technol. 162 (2018) 170–179. http://dx.doi.org/10.1016/J.COMPSCITECH.2018.04.036.
[3] C.J. Lee, S.H. Kwon, H.J. Choi, K.H. Chung, J.H. Jung, Enhanced magnetorheological performance of carbonyl iron/natural rubber composite elastomer with gamma-ferrite additive, Colloid Polym. Sci. 296 (2018) 1609–1613. http://dx.doi.org/10.1007/s00396-018-4373-0.
[4] G.V. Stepanov, S.S. Abramchuk, D.A. Grishin, L.V. Nikitin, E.Y. Kramarenko, A.R. Khokhlov, Effect of a homogeneous magnetic field on the viscoelastic behavior of magnetic elastomers, Polymer (Guildf). 48 (2007) 488–495. http://dx.doi.org/10.1016/J.POLYMER.2006.11.044.
[5] A. Boczkowska, S. Awietjan, Microstructure and properties of magnetorheological elastomers, in: A. Boczkowska (Ed.), Adv. Elastomers – Technol. Prop. Appl., InTechOpen, London, 2017 595.
[6] X. Wang, F. Gordaninejad, Magnetorheological materials and their applications, in: H.-J. rg, S. Mohsen Shahinpoor (Eds.), Intell. Mater., The Royal Society of Chemistry, Cambridge, 2008.
[7] W.H. Li, X.Z. Zhang, H. Du, A. Öchsner, L.F.M. da Silva, H. Altenbach, Magnetorheological elastomers and their applications, in: P.M. Visakh, S. Thomas, A.K. Chandra, A.P. Mathew (Eds.), Adv. Elastomers I Blends Interpenetr. Networks, Springer, Berlin, 2013.
[8] L. Chen, X. Gong, W. Jiang, J. Yao, H. Deng, W. Li, Investigation on magnetorheological elastomers based on natural rubber, J. Mater. Sci. 42 (2007) 5483–5489. http://dx.doi.org/10.1007/s10853-006-0975-x.
[9] J. Kaleta, M. Królewicz, D. Lewandowski, Magnetomechanical properties of anisotropic and isotropic magnetorheological composites with thermoplastic elastomer matrices, Smart Mater. Struct. 20 (2011) 85006, http://dx.doi.org/10.1088/0964-1726/20/8/085006.
[10] S. Raa Khimi, K.L. Pickering, B.R. Mace, Dynamic properties of magnetorheological elastomers based on natural rubber and iron sand, J. Appl. Polym. Sci. 132 (2014) 41506, http://dx.doi.org/10.1002/app.4150610.1002/APP.41506 (1–13).
[11] W.H. Li, M. Nakano, Fabrication and characterization of PDMS based magnetorheological elastomers, Smart Mater. Struct. 22 (2013) 55035, http://dx.doi.org/10.1088/0964-1726/22/5/055035.
[12] I.A. Perales-Martínez, L.M. Palacios-Pineda, L.M. Lozano-Sánchez, O. Martínez-Romero, J.G. Puente-Cordova, A. Elías-Zúñiga, Enhancement of a magnetorheological PDMS elastomer with carbonyl iron particles, Polym. Test. 57 (2017) 78–86. http://dx.doi.org/10.1016/j.polymertesting.2016.10.029.
[13] J. Li, X. Gong, Z. Xu, W. Jiang, The effect of pre-structure process on magnetorheological elastomer performance, Int. J. Mater. Res. 99 (2008) 1358–1364.
[14] J.S. An, S.H. Kwon, H.J. Choi, J.H. Jung, Y.G. Kim, Modified silane-coated carbonyl iron/natural rubber composite elastomer and its magnetorheological performance, Compos. Struct. 160 (2017) 1020–1026. http://dx.doi.org/10.1016/j.compstruct.2016.10.128.
[15] H.S. Jung, S.H. Kwon, H.J. Choi, J.H. Jung, Y.G. Kim, Magnetic carbonyl iron/natural rubber composite elastomer and its magnetorheology, Compos. Struct. 136 (2016) 106–112. http://dx.doi.org/10.1016/j.compstruct.2015.10.008.
[16] J. Ubaidillah, A. Sutrisno, S.A. Purwanto, Mazlan, Recent progress on magnetorheological solids – materials, fabrication, testing, applications, Adv. Eng. Mater. (2014), http://dx.doi.org/10.1002/adem.201400258.
[17] M. Yu, S. Qi, J. Fu, M. Zhu, D. Chen, Understanding the reinforcing behaviors of polyaniline-modified carbonyl iron particles in magnetorheological elastomer based on polyurethane/epoxy resin IPNs matrix, Compos. Sci. Technol. 139 (2017) 36–46. http://dx.doi.org/10.1016/j.compscitech.2016.12.010.
[18] J. Wu, X. Gong, L. Chen, H. Xia, Z. Hu, Preparation and characterization of isotropic polyurethane magnetorheological elastomer throughin situpolymerization, J. Appl. Polym. Sci. 114 (2009) 901–910. http://dx.doi.org/10.1002/app.30563.
[19] X. Qiao, X. Lu, X. Gong, T. Yang, K. Sun, X. Chen, Effect of carbonyl iron concentration and processing conditions on the structure and properties of the thermoplastic magnetorheological elastomer composites based on poly (styrene-b-ethylene-co-butylene-b-styrene) (SEBS), Polym. Test. 47 (2015) 51–58. http://dx.doi.org/10.1016/j.polymertesting.2015.08.004.
[20] J. Ubaidillah, A. Sutrisno, S.A. Purwanto, Mazlan, Recent progress on magnetorheological solids: materials, fabrication, testing, and applications, Adv. Eng. Mater. 17 (2015) 563–597. http://dx.doi.org/10.1002/adem.201400258.
[21] Y. Sun, Y. Wang, J. Yao, L. Gao, D. Li, Y. Liu, Highly magnetic sensitivity of polymer nanocomposite hydrogels based on magnetic nanoparticles, Compos. Sci. Technol. 141 (2017) 40–47. , http://dx.doi.org/10.1016/J.COMPSCITECH.2017.01.006.
[22] W.D. Armstrong, A. Boczkowska, S. Awietjan, K. Babski, R. Wroblewski, M. Leonowicz, Effect of the processing conditions on the Microstructure of Urethane Magnetorheological Elastomers, vol. 6170, 2006. p. 61700R http://dx.doi.org/10.1117/12.651668.
[23] R.K. Roy, A Primer on The Taguchi Method, 2nd ed., Society of Manufacturing Engineers, Dearborn, 2010.
[24] D.C. Jiles, Theory of the magnetomechanical effect, J. Phys. D: Appl. Phys. 28 (1995) 1537 http://stacks.iop.org/0022-3727/28/i=8/a=001.
[25] A. Fuchs, Q. Zhang, J. Elkins, F. Gordaninejad, C. Evrensel, Development and characterization of magnetorheological elastomers, J. Appl. Polym. Sci. 105 (n.d.) 2497–2508, doi:10.1002/app.24348.

[26] S. Raa Khimi, K.L. Pickering, Investigation and modelling of damping mechanisms of magnetorheological elastomers, J. Appl. Polym. Sci. 133 (2015) 43247, http://dx.doi.org/10.1002/app.4324710.1002/APP.43247 (1–11).
[27] M. Rendek, A. Lion, Amplitude dependence of filler-reinforced rubber: experiments, constitutive modelling and FEM – implementation, Int. J. Solids Struct. 47 (2010) 2918–2936.
[28] Y. Wang, X. Zhang, J. Oh, K. Chung, Fabrication and properties of magnetorheological elastomers based on CR/ENR self-crosslinking blends, Smart Mater. Struct. 24 (2015) 95006, http://dx.doi.org/10.1088/0964-1726/24/9/095006.